J. Mt. Sci. (2026) 23(5): 1865-1883 e-mail: jms@imde.ac.cn http://jms.imde.ac.cn
https://doi.org/10.1007/s11629-025-0306-9

Original Article

Modeling of the largest snow avalanche tragedy in the Western Carpathians (Veľká Fatra Mountains – Slovakia)

Matej MASNÝ[1*] https://orcid.org/0000-0003-1043-0525; e-mail: matej.masny@umb.sk

Pavel KRAJČÍ[2] https://orcid.org/0000-0002-1155-5680; e-mail: krajci.palo@gmail.com

**Corresponding author*

1 Department of Geography and Geology, Faculty of Natural Sciences, Matej Bel University, Tajovského 40, 974 01 Banská Bystrica, Slovakia

2 Avalanche Prevention and Education Center, Mountain Rescue Service of Slovakia, Žiar 366, 032 05 Žiar, Slovakia

Citation: Masný M, Krajčí P (2026) Modeling of the largest snow avalanche tragedy in the Western Carpathians (Veľká Fatra Mountains – Slovakia). Journal of Mountain Science 23(5). https://doi.org/10.1007/s11629-025-0306-9

Abstract: On February 6, 1924, a catastrophic snow avalanche struck the settlement of Rybie in the Veľká Fatra Mountains, remaining the deadliest avalanche disaster on record in Slovakia and the entire Western Carpathians, with 18 fatalities. Historical documentation offers limited quantitative data on the event's parameters, including release zone locations and snow depths, although the positions of destroyed buildings can still be partially identified in the field. Leveraging recent advances in high-resolution terrain data (e.g., LiDAR), GIS-based tools for identifying potential release areas (PRA), and dynamic simulation models (AvaFrame and RAMMS::Avalanche), this study performs a back-calculation of the 1924 avalanche. A series of simulations were conducted based on delineated PRAs and analyzed against a critical destructive pressure threshold of 20 kPa at the locations of the former buildings. The results identify an avalanche with a crown height of at least 1.6 m as the most probable scenario. These findings contribute to the reassessment of the site's future avalanche vulnerability and provide a methodological contribution to avalanche modeling and historical accident reconstruction.

Keywords: Snow avalanche reconstruction; Potential release area; AvaFrame; RAMMS::Avalanche; Veľká Fatra Mountains

Received: 13-Nov-2025
Revised: 24-Mar-2026
Accepted: 30-Apr-2026

1 Introduction

The adage "The more you know about the past, the better prepared you are for the future," often attributed to Theodore Roosevelt (1858–1919), holds true for catastrophic events such as the avalanche that struck the Veľká Fatra Mountains in 1924. Occurring on the night of February 6–7 in the Hornojelenecká Valley, the avalanche affected the settlement of Rybie (formerly Rybô) and claimed 18 lives, including 15 children. It destroyed one brick house, two wooden houses, and several farm buildings, while severely damaging two additional structures (Karpathen-Post 1924).

Snow avalanches are always the result of the complex interplay between climatic factors, current meteorological conditions, and local terrain characteristics (including slope gradient and aspect, slope shape curvature, elevation and land cover). Avalanche accidents are often preceded by intricate meteorological phenomena, such as the combination of intense precipitation, strong winds, and elevated temperatures (Schweizer et al. 2009; Eckert et al. 2010). These meteorological phenomena have a significant impact on the conditions of snowpack and their occurrence is currently reported mainly in the context of global climate change (Eckert et al. 2024;

Mayer et al. 2024; Ortner et al. 2025). However, the terrain characteristics can be regarded as fundamental prerequisites for the potential occurrence of avalanche risk (Valero et al. 2015; Liščák et al. 2017). In addition to static factors such as slope and aspect, this also includes properties of the land cover that influence surface roughness. This represents a relatively dynamic factor, for example, in the form of targeted deforestation or reforestation (García-Hernández et al. 2017; Bergua et al. 2019). In general, it can be stated that the tragic events in the settlement of Rybie occurred because of a combination of all the factors mentioned above.

The size and severity of the event can be used as a basis for further examination of avalanche vulnerability in this area, as well as for evaluating the effectiveness of reforestation and other mitigation measures applied for avalanche protection. However, a precise reconstruction of this largest recorded event is required first. That is the reason we want to collect all available historical data and records and combine it with modern methods and data sources to reconstruct this event as precisely as possible. In the last 20 years several papers dealt with this avalanche event. Bartík and Richnavský (2015) reconstructed the avalanche with ELBA+ and RAMMS model, but they used the digital terrain model (DTM) derived from an old topographic map digitalized from the paper version with scale 1:10 000. The release area was estimated by empirical subjective methods, because more accurate DTM and release area calculation methods were not available at that time. Vojtek (2015) and Mikulova et al. (2024) were focused on the climatic, synoptic and meteorological side of the event. These papers are a very good partial base, but the complex work combining all the aspects was missing.

The main objective of this study is the back-calculation of the avalanche event using new data sources and tools, historical data, and the results of previously conducted studies. Particular emphasis is placed on a new digital terrain model (DTM) derived from LiDAR data. All relevant inputs related to the weather preceding the event are also summarized, including historical meteorological records from nearby stations and the reanalyzed synoptic situation from NOAA/CIRES/DOE version 3 (Slivinski et al. 2019), as used and validated by Mikulova et al. (2024). The influence of weather conditions on snow cover stratigraphy is subsequently analyzed. Based on DTM data, historical aerial imagery, and historical meteorological records, potential release zones are identified using an automatic algorithm. These data are then utilized in two different dynamic avalanche simulation tools (AvaFrame and RAMMS::Avalanche). The simulations were conducted in two separate steps, as a preceding avalanche had a significant impact on the local terrain prior to the main avalanche event. Finally, the simulation results are validated against the locations of the destroyed buildings, which represent the maximum extent of the avalanche event. The simulation results are also compared with historical records describing additional deposit parameters. The individual steps and their sequence are graphically illustrated in a schematic diagram summarizing the methodological workflow (Fig. 1).

Attention is focused not only on the avalanche's reach but also on its destructive effects at the site of the tragedy. This, in turn, allows for the determination of the minimum average release depth that generated the avalanche. The analysis of destructive forces at the sites of the affected buildings, combined with the analysis of the deposit extent, makes it possible to

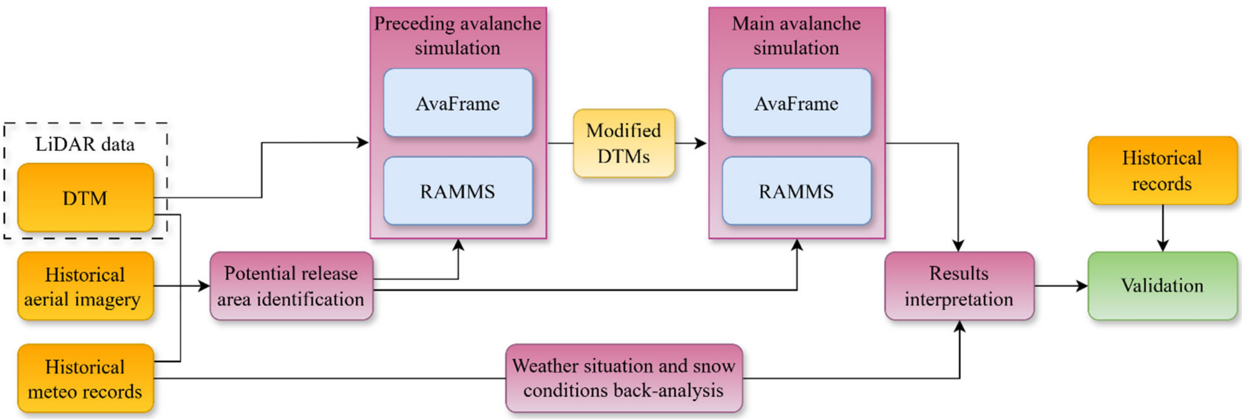

Fig. 1 Methodological workflow diagram.

identify the most probable scenario of this tragic event. Furthermore, the models allow for a retrospective analysis of avalanche parameters that are not included in historical records.

2 Study Area

2.1 Area of avalanche disaster

The Hornojelenecká Valley is part of the Krížna massif (1,574 m a.s.l.), which represents the highest peak of the Veľká Fatra Mountains. The area is in central Slovakia. The valley is oriented southeast and forms the catchment area of the Rybie Stream. The mouth of the valley lies at an elevation of 580 m a.s.l., at the confluence of the Rybie Stream and the Starohorský Stream. Within the valley are three settlements (Horný Jelenec, Valentová, and Rybie) which are administratively part of the municipality of Staré Hory. The settlement of Rybie (historically known as Rybô) is the highest situated among them, with its central area located at an elevation of 690 meters a.s.l. (Fig. 2).

This area has a long history of grazing and logging. Shepherds and woodcutters in the Veľká Fatra significantly affected the land cover of the ridge zone. Through burning and felling, they cleared the forest from slopes and summits, reducing the forest boundary to the beech forest zone. The expansion of pastures also significantly influenced the occurrence of mountain pine, with only isolated patches mostly preserved, typically in inaccessible areas of rocky ridges and terraces. Pressure on forests also increased from the valleys. The mining and processing industries created a continuous demand for charcoal. From approximately the second half of the 16th century, mining and charcoal-production settlements were established in the Veľká Fatra valleys, such as Turecká, Prášnica, Valentová, and the settlement of Rybie. The inhabitants thus came into direct contact with the natural phenomenon of avalanches (Longauer et al. 2015).

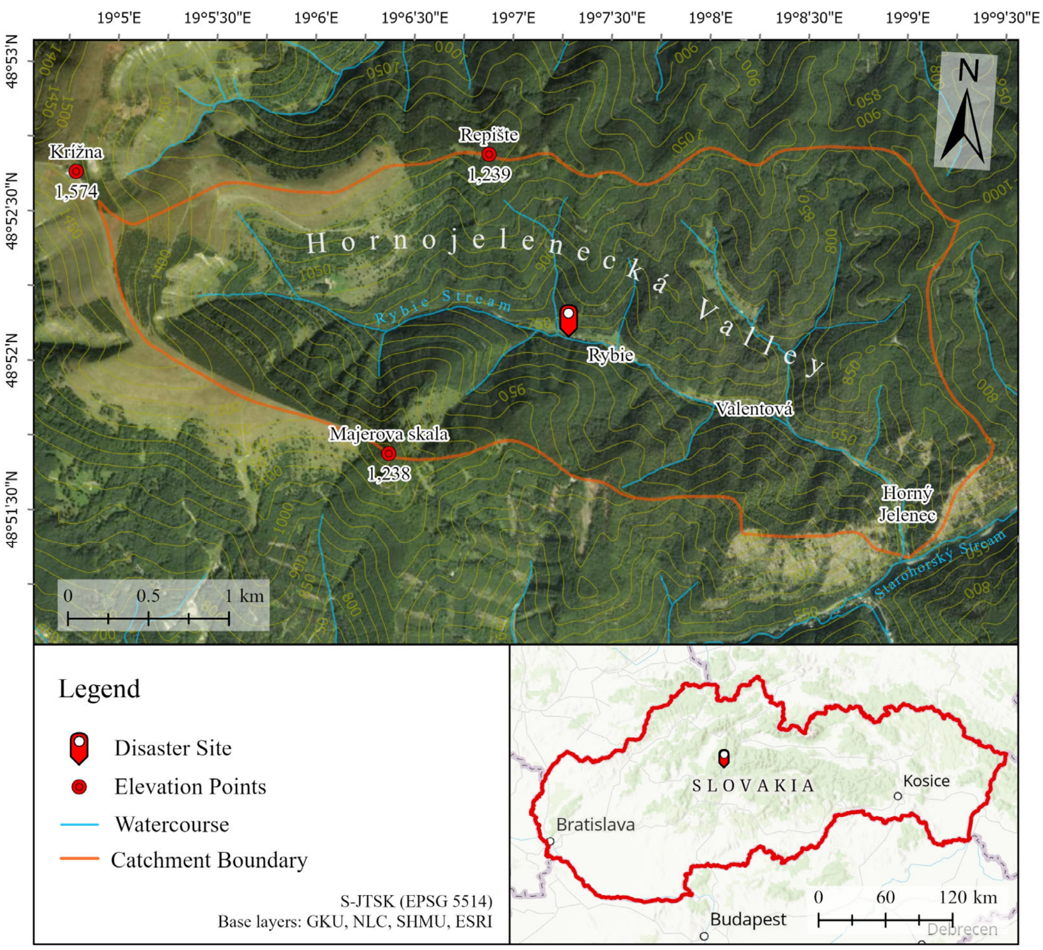

Fig. 2 Location of the disaster site and delineation of the Hornojelenecká Valley.

2.2 Historical records of the avalanche event

Contemporary documentation of this tragic event is therefore considerably limited. In addition to the aforementioned loss of human lives and damaged buildings, the records also included information about the avalanche path and the resulting deposit. These data are highly valuable for reconstructing the event; however, when compared to today's high-precision measurement methods, they should be interpreted with caution. The primary sources include archival records from the municipality of Staré Hory, as well as documents from the Museum of Forestry and Wood Technology and the Avalanche Prevention and Education Center. Most previously published studies on this event also relied on these sources (e.g., Bukovčan 1960; Longauer 2015; Bartík and Richnavský 2015). Based on these data, the basic parameters of the avalanche are summarized in the overview presented in Table 1.

Historical records also contain photographic documentation, both immediately after the event (Fig. 3a) and several months later (Fig. 3b). However, these photographs were not taken using the systematic approach to event documentation that is standard today. The image quality of this photographic documentation may be considerably limited.

In the context of historical records, contemporary periodicals are of great importance, as they may provide near-immediate information. A detailed account of this tragic event can be found in the *Karpathen-Post*, a periodical published in Kežmarok (historically known as Käsmark in Slovakia), which ran from 1880 to 1942. This publication likely served the German-speaking community in the Carpathian region at the time, covering local news, culture, and regional topics. The original article, *Der Lawinensturz bei Altgebirg*, was published on March 1, 1924, in Volume 45 (Issue No. 9) on page 2. The entire issue is available in the DiFMOE digital library.

Table 1 Basic avalanche parameters according to historical records

Parameter	Value
Avalanche length (m)	2,500
Avalanche deposit length (m)	1,500
Avalanche deposit height (m)	10–25
Area of forest affected (100-120-year-old coniferous forest) (ha)	4
Number of affected buildings	5

In addition to numerical data on avalanche parameters, historical records also provide an important reference to a smaller avalanche that occurred prior to the main event. The cited issue of the *Karpathen-Post* specifically mentions an avalanche released from the side valley in the Rizne locality. The Rizne locality is situated on the left side of the main axis of the Hornojelenecká Valley (Fig. 4) and represents a side valley leading to the elevation point Repište (1,239 m a.s.l.). This avalanche occurred a few days before the main event. Its length was estimated at approximately 1 km and its width at 50 –100 m. In the axis of the main valley, it reportedly formed a deposit about 8 m high, creating a barrier above the settlement

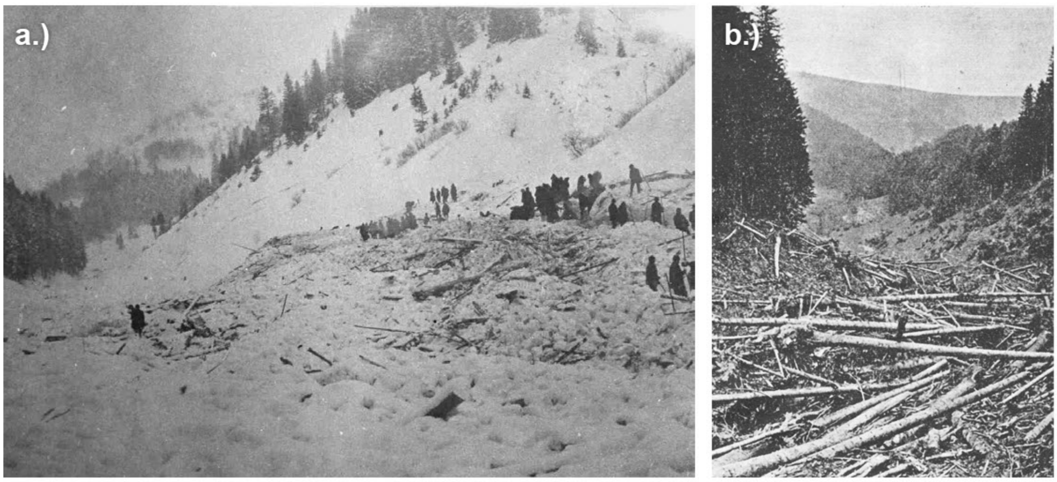

Fig. 3 Example of photographic documentation of the event. (a) Rescue operations on February 7, 1924, a few hours after the avalanche event. (b) Timber debris from the avalanche deposit. The photograph likely shows conditions several months after the event; however, the exact date of the image is unknown. (Source: Archive of the Museum of Forestry and Wood Technology).

of Rybie that may have mitigated the impact of the subsequent avalanche. This information proved to be very important for further modeling.

2.3 Location of destroyed buildings and the maximum avalanche runout

The affected buildings were never rebuilt due to the persistent avalanche hazard. Regrettably, the exact plans and locations of the buildings are not currently available, and this issue requires further research, particularly from archival and historical sources. The only known information is that three buildings were destroyed, one brick and two wooden, while two additional buildings were severely damaged. The extent and parameters of the avalanche deposit at the site of the affected buildings cannot be precisely determined. However, fragments of the foundation of one of these buildings can still be identified in the field. The site is now covered by secondary succession, primarily in the form of shrubs and low trees (Fig. 4). For this reason, its position was surveyed using a GNSS device prior to the start of the vegetation period in early April 2025. This generalized point represents the sole precise location where the avalanche caused destructive impact on the buildings and is therefore crucial for further modeling. Higher up the slope, a memorial site with a cross was established by the local authorities to commemorate the tragic events (Fig. 4).

2.4 Meteorological records

Systematic weather observations in the former territory of Czechoslovakia have a long tradition. They

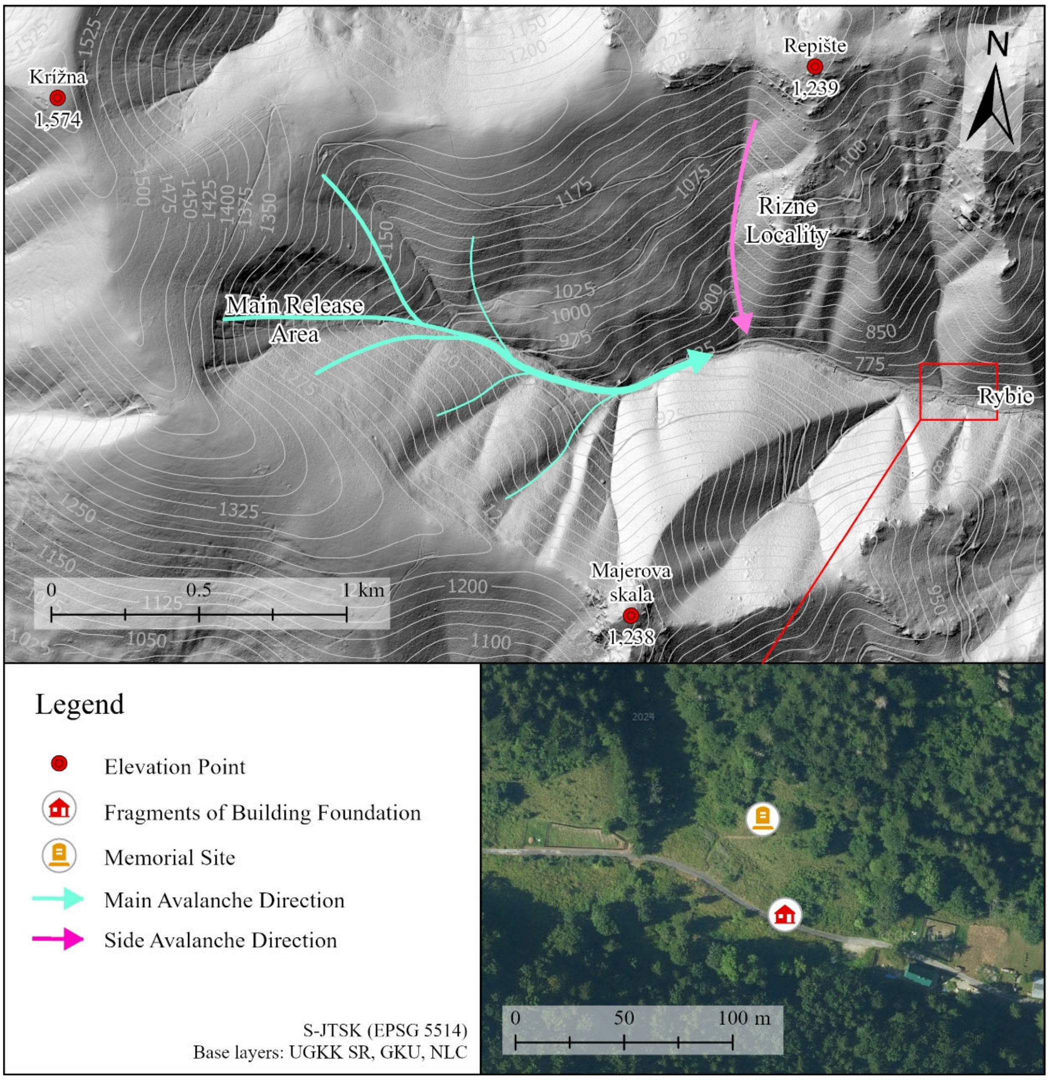

Fig. 4 Schematic of avalanche progression and the location of preserved building foundations.

were typically conducted by field observers and recorded daily (Fig. 5). Selected meteorological parameters from the nearest weather stations can therefore be used to reconstruct the weather conditions preceding the tragic avalanche event. These parameters include air temperature, cloudiness, and wind direction, measured three times per day (07:00, 14:00, and 21:00), as well as precipitation, measured once daily (07:00).

Data from two meteorological stations were considered. The closest station to the study area with records available from 1924 is Staré Hory, located just 4 km south of the Rybie area at an elevation of 480 m a.s.l. This station is well suited for estimating general weather conditions, particularly cloudiness and precipitation occurrence. Its main limitation is its low elevation relative to the avalanche release zone, located at approximately 1,400 m a.s.l. Due to orographic effects, a significantly higher amount of precipitation can be expected at the release site. Conversely, air temperature is likely to be much lower there, especially during clear weather.

The second station used for data collection was Magurka, located approximately 26 km northeast of the study area. Its elevation is approximately 1,030 m a.s.l., much closer to the altitude of the avalanche release zone. This station is more suitable for estimating air temperature and compared to Staré Hory, allows for the avoidance of temperature inversion effects. A limitation of this station is its location on the northern side of the Low Tatras, where climatic conditions are influenced by the mountain range. When precipitation comes from the south, this site records much less precipitation than Staré Hory and the Rybie area. Conversely, when precipitation comes from the northwest, this station serves as a better indicator of snow accumulation for the Rybie area.

3 Methods and Tools for Avalanche Event Modeling

3.1 Weather conditions and dry snow metamorphism

The combination of data from the two aforementioned stations enabled a reliable reconstruction of the weather conditions that influenced the course of this catastrophic event. Retrospective analyses from the NOAA–CIRES–DOE Twentieth Century Reanalysis, version 3 (Slivinski et al. 2019), were used to examine the synoptic situation. This third version of the Twentieth Century Reanalysis was developed by the National Oceanic and Atmospheric Administration (NOAA), the Cooperative Institute for Research in Environmental Sciences (CIRES) at the University of Colorado Boulder, and the U.S. Department of Energy (DOE). It employs a higher-resolution model, assimilates a larger set of observations, and incorporates an improved data assimilation system.

Under the influence of atmospheric and temperature conditions, the snowpack undergoes continuous transformations. If it remains entirely below the freezing point and contains no liquid water, this process is referred to as dry snow metamorphism. In seasonal snowpacks, ground temperatures typically remain near 0°C throughout the winter, as the ground gradually releases residual heat accumulated during warmer months. This upward geothermal heat flux, in contrast to the colder ambient air typical of winter, establishes a vertical temperature gradient within the snowpack. Under conditions of a low temperature gradient, snow crystals evolve into rounded grains through a process known as equi-temperature metamorphism (Adams and Brown 1983; Colbeck 1982). During this process, the sharp edges of fresh snowflakes gradually sublimate and redeposit as water vapor, causing the grains to become smaller, rounder, and more tightly bonded. As the grains become more rounded, the snowpack becomes denser, stronger, and more cohesive.

A temperature gradient in the snowpack produces a corresponding water vapor pressure gradient, resulting in a flux of water vapor from warmer to colder regions. This vapor flux toward colder regions can lead to the formation of large, faceted crystals, which are only weakly bonded to the surrounding snow. The processes involved in dry snow metamorphism are critical for understanding avalanche formation, as avalanches often initiate in weak layers within the snowpack. Ice lenses—layers of solid ice formed within the snowpack due to freezing rain or melt-freeze events—also play a significant role in avalanche formation (Jamieson et al. 2001). The critical temperature gradient required for the formation of faceted crystals in alpine snow is approximately 1°C per 10 cm. (LaChapelle and Armstrong 1977; McClung and Schaerer 1993). Based on available historical meteorological data, a back-analysis of snow conditions was conducted to assess the potential for faceted snow formation.

3.2 Data about terrain and land cover

For the terrain input data, the fifth-generation digital terrain model (DTM 5.0) was used. The spatial resolution of DTM 5.0 is 1 m × 1 m. It was generated from point clouds obtained through airborne laser scanning (LiDAR). The point cloud data were acquired using a Riegl LMS-VQ780i scanner mounted on a Cessna 207 aircraft. Data acquisition was conducted during the leaf-off period, with an average point density of 5.9 points per square meter. Classification class no. 02, “Relief (Ground)”, was used as the input class. DTM 5.0 is available for the entire territory of Slovakia and was produced under the supervision of

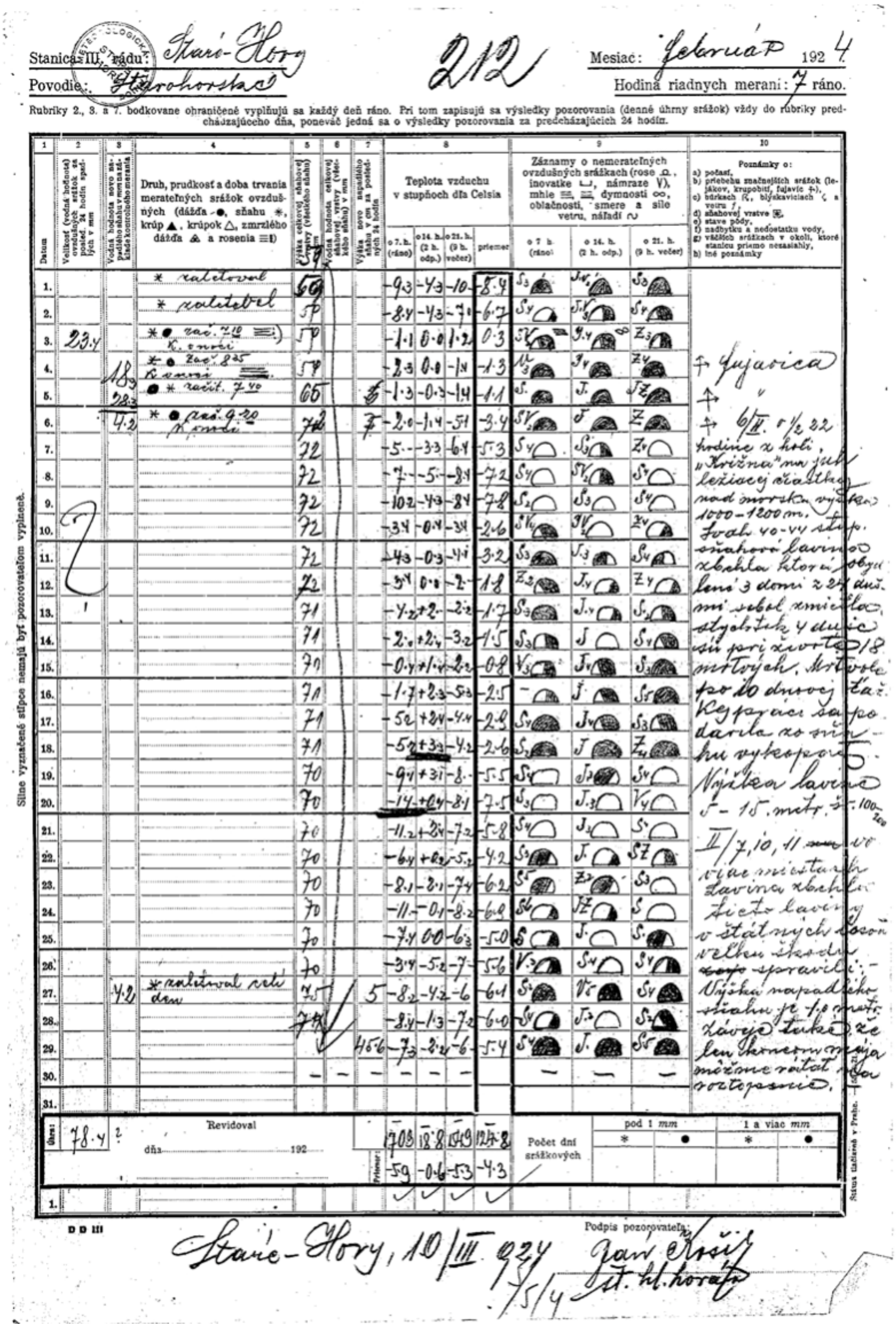
Stanica III. rádu: Staré Hory
Povodie: Starohorská
212
Mesiac: február 1924
Hodina riadnych meraní: 7 ráno.
Rubriky 2., 3. a 7. bodkovane ohraničené vyplňujú sa každý deň ráno. Pri tom zapisujú sa výsledky pozorovania (denné úhrny zrážok) vždy do rubriky predchádzajúceho dňa, ponevač jedná sa o výsledky pozorovania za predchádzajúcich 24 hodín.
Datum
Veľkosť (vodná hodnota) ovzdušných zrážok za posled. 24 hodín spadlých v mm
Vodná hodnota novo napadlého snehu
Druh, prudkosť a doba trvania merateľných zrážok ovzdušných (dážď, snehu, krúp, krúpok, zmrzlého dážďa a rosenia)
Teplota vzduchu v stupňoch dľa Celsia
o 7. h. (ráno) | o 14. h. (2 h. odp.) | o 21. h. (9 h. večer) | priemer
Záznamy o nemerateľných ovzdušných zrážkach (rose, inovatke, námraze, mhle, dymnosti, oblačnosti, smere a sile vetru, náraďí)
o 7 h. (ráno) | o 14. h. (2 h. odp.) | o 21. h. (9 h. večer)
Poznámky o: a) počasí, b) priebehu značnejších zrážok (lejákov, krupobití, fujavíc), c) búrkach, blýskaviciach a vetru, d) snehovej vrstve, e) stave pôdy, f) nadbytku a nedostatku vody, g) väčších zrážok v okolí, ktoré stanicou priamo nezasiahly, h) iné poznámky
Sčot
Revidoval dňa 192
Priemer
Počet dní zrážkových
pod 1 mm | 1 a viac mm
Silne vyznačené stĺpce nemajú byť pozorovateľom vyplnené.
D D III
Podpis pozorovateľa:
Staré Hory, 10/III. 924
Jan Krsiž st. hl. horár

the Geodetic and Cartographic Institute Bratislava (GKU).

For the purposes of the subsequent modeling process, a digital terrain model with a spatial resolution of 5 m × 5 m was derived from the original DTM 5.0. This was performed in the ArcGIS Pro (Esri) software environment using bilinear interpolation.

Historical aerial imagery represents the most accurate record of actual land cover at a given time and provides valuable information on land use. Unlike cartographic products, these images are not affected by generalization. For the study area, the earliest available aerial photographs date back to 1950 (Fig. 6), which is 26 years after the avalanche event. This time span is insufficient for the forest to have reached full maturity. Therefore, the aerial imagery can be used to approximately identify forested areas affected by the avalanche, which may help verify the simulated avalanche trajectory. Moreover, no reforestation projects are known to have taken place in the study area during the 1930s or the World War II period. Consequently, the 1950 aerial images can be considered sufficiently reliable for reconstructing the probable land cover at the time of the 1924 avalanche event. The first experimental avalanche barriers in the locality were not established until 1956 (Longauer et al., 2015). At present, the study area has been significantly altered by vegetation growth resulting from reforestation (Fig. 6). The historical aerial images used in this study were processed into an orthophotomosaic provided by the Technical University in Zvolen (© GEODIS SLOVAKIA, s.r.o.; PHOTOMAP, s.r.o.; © Topographic Institute Banská Bystrica).

3.3 Potential release areas

In the past, the estimation of avalanche release zones in hazard mapping was based on empirical observations of actual avalanches by experts, for example, in the avalanche cadastre of Slovakia (Kňazovický 1979). The development of geographic information systems (GIS) and digital terrain models (DTMs) subsequently led to increased scientific interest in the automatic delineation of avalanche release areas. These algorithms are based on terrain characteristics such as slope, aspect, and curvature derived from DTMs (Maggioni and Gruber 2003; Bühler et al. 2013).

The concept of Potential Release Areas (PRA), introduced by Veitinger et al. (2016), represents an improved approach to the automatic estimation of the maximum extent of avalanche starting zones. The main inputs include terrain and vegetation parameters. Veitinger et al. (2016) incorporated roughness and wind shelter into the algorithm and combined all inputs using fuzzy logic methods. Sharp (2018) further improved the approach by incorporating forest density as a fuzzy logic variable, which had previously been treated as a binary parameter – effectively classifying areas as either "forested" or "non-forested." In the binary approach, any forested area was excluded from further processing by the PRA model and labeled as

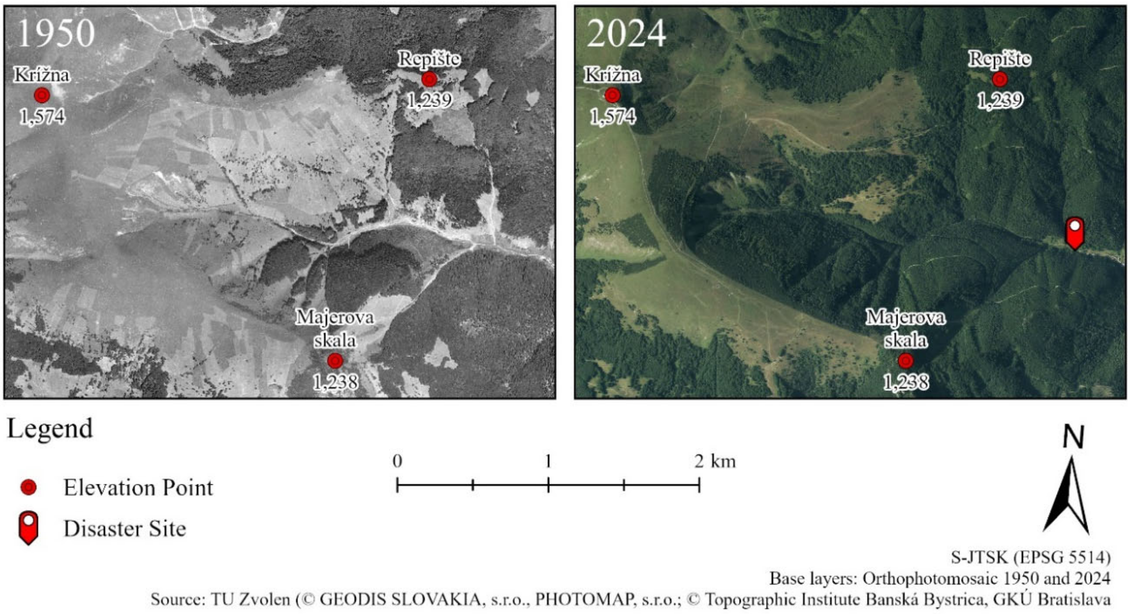

Fig. 6 Illustration of land cover change in the upper part of the Hornojelenecká Valley.

non-PRA. Unlike binary logic, fuzzy logic does not restrict inputs to yes-or-no values; instead, it allows for continuous degrees of membership. This method accounts for variations in forest density and treats them with equal importance to other factors such as surface roughness, slope angle, and wind shelter.

In recent years, this improved method has been used for avalanche terrain classification, for example, in Avalanche Terrain Exposure Scale (ATES) mapping (Toft et al. 2024a; Sykes et al. 2024). The modified algorithm (ATES version 2.0) was used in this study. It is an open-source tool available online (Toft 2024b). The algorithm was applied to the study area using the previously described 5 m × 5 m spatial resolution. This resolution is widely used in avalanche modeling and is considered appropriate for representing snow-on-terrain conditions (Miller et al. 2022). In this case, the avalanche was observed to have occurred on a snow-covered surface, as confirmed by historical records. A finer resolution (<2 m) is generally recommended for steep, rugged terrain and small avalanches (Miller et al. 2022), which was not the case for this event. The 5 m × 5 m resolution was also selected because it is recommended for use in the AvaFrame and RAMMS modules employed in this study. This resolution is determined based on local conditions and is suitable for simulating medium to large-scale dense-flow snow avalanches. The output was generated as vector polygons representing potential release areas, which were subsequently incorporated into the simulation process.

3.4 AvaFrame

The Open Avalanche Framework (AvaFrame) is an open-source framework (licensed under the European Union Public License – EUPL) for avalanche simulation, designed to replicate and streamline current simulation procedures and models. The AvaFrame environment (version 1.13.1) incorporates several computational modules. For the purposes of this study, the DFA-Kernel module was employed.

The DFA-Kernel module (com1DFA) is designed for simulating dense-flow avalanches (DFA). It is implemented in Python and Cython and is based on the C++ SamosAT framework (Snow Avalanche Modeling and Simulation Advanced Technologies), developed by the Austrian government in collaboration with AVL List GmbH in Graz. The SamosAT friction model represents a modification of classical models, such as the Voellmy friction model. The module performs calculations using thickness-integrated governing equations, which are numerically solved using the smoothed particle hydrodynamics (SPH) method. Dense-flow avalanche simulations can be performed for various release area scenarios, with or without entrainment and resistance zones. The simulation process is controlled via a configuration file, which can be modified to adjust default settings and allows for batch simulations across multiple parameter variations. The configuration included with this module has been tested and successfully applied in avalanche hazard mapping in Austria. The com1DFA module is calibrated for simulating medium- to large-scale dense-flow snow avalanches (Oesterle et al., 2025). The input data consist of a DTM and polygons representing avalanche release areas (PRA), with the option to define release depth (crown height). The outputs include raster datasets of peak pressure, flow thickness, and flow velocity. An additional important output is the deposit thickness model.

3.5 RAMMS::Avalanche

Rapid Mass Movement Simulation (RAMMS) is a two-dimensional numerical simulation model developed by the WSL Institute for Snow and Avalanche Research SLF (Zurich, Switzerland). The model is designed for the simulation of avalanches, debris flows, and rockfall. Within this study, the RAMMS::Avalanche (version 1.8.0) module was applied.

RAMMS::Avalanche uses depth-averaged equations to predict the flow heights and slope-parallel velocities of flows composed of fast-moving snow particles suspended in an interstitial fluid (air). The friction law is based on the Voellmy–Salm–Gubler (VSG) friction model. The model divides the frictional resistance into two components: a dry-Coulomb-type friction (coefficient μ) proportional to the normal stress, and a velocity-squared drag, or viscous-turbulent, friction (coefficient ξ). In RAMMS::Avalanche, the friction parameters can be set as either constant or spatially variable within the computational domain. The tool also allows for automatic calculation of friction values based on topography and elevation using a DTM, depending on the avalanche's return period and magnitude (Christen et al. 2010; Martini et al. 2023). In addition to the DTM, a vector layer of PRAs is included as a fundamental input, with the option to define the release depth (crown height). As with the AvaFrame outputs, the results are raster models representing maximum pressure, flow velocity, flow height, and deposit thickness.

4 Results

4.1 Weather situation and snow conditions back-analysis

The winter season of 1923/24 was characterized by exceptionally abundant snowfall and avalanche activity in the mountains of Slovakia. During the first half of January, however, snow cover was limited, with approximately 20 cm recorded at the Staré Hory station and about 15 cm at the Magurka station. Subsequently, heavy precipitation associated with southerly airflow was recorded. This resulted in an additional 30 cm of snow at the Staré Hory station. In contrast, only a minor increase was observed at the Magurka station due to the aforementioned mountain barrier (Fig. 7).

On January 23, the air temperature at the 850 hPa level gradually decreased to −15°C and further dropped to −20°C by January 24. At the Magurka station (1030 m a.s.l.), temperatures decreased to −10°C. From January 25 to 28, the weather in Central Europe was influenced by a large high-pressure system, and cold air was advected into the region from the northeast. At the 850 hPa level, air temperatures of −15°C on January 25 and approximately −7°C on January 28 were recorded. In the valleys, temperatures as low as −17°C at the Magurka station and −13°C at the Staré Hory station were observed.

Cyclonic conditions with precipitation from the northwest were observed on January 28 and 29, while air temperatures at the 850 hPa level ranged from −7°C to −10°C. From January 30 to February 1, anticyclonic conditions prevailed, with no precipitation recorded and temperatures at the 850 hPa level remaining around −10°C.

The weather between February 2 and 6, 1924, is considered to have played a decisive role in avalanche formation. A deepening low-pressure system over the Baltic States, associated with a frontal system over Slovakia, resulted in a dominant northwesterly cyclonic situation. Heavy snowfall accumulated on the northwestern (windward) slopes of the mountains, including the Veľká Fatra ridge and the Krížna massif, as a result of orographic uplift. Snow was readily transported by northwesterly winds to the leeward side due to the absence of trees at the mountain summits, leading to the development of a deep snowpack on the eastern slopes. Temperatures at the 850 hPa level remained below freezing from February 2 to 5 (Mikulova et al. 2024).

Snow stratigraphy is strongly influenced by temperature and other weather conditions, as discussed previously. Basic calculations of temperature gradients within the snowpack were performed for three daily observation times (07:00, 14:00, and 21:00). The snowpack was assumed to be a uniform layer due to insufficient data for more detailed modeling. The temperature at the snow–soil interface was approximated as 0°C.

Two main periods were identified from mid-January until the day of the avalanche event. The first period, from January 16 to 21, was characterized by low temperature gradients and greater snow accumulation on the southern side of the mountains (Staré Hory station). These gradients were insufficient for faceting (i.e., the formation of faceted snow grains). In contrast, the northern side (Magurka station) had less snow, so even temperatures around −3°C were sufficient to produce a temperature gradient exceeding 1°C per 10 cm.

The situation changed under cold, dry conditions from January 21 to 29. During this period, the highest temperature gradients were observed, exceeding 2°C per 10 cm at both stations. Minimum temperatures at the Magurka station dropped below −15°C at an elevation of approximately 1,000 m a.s.l. Based on these observations, slightly lower temperatures can be expected at the avalanche crown elevation of 1,400 m a.s.l. Therefore, even with a snow depth exceeding 150 cm, the temperature gradient likely exceeded 1°C per 10 cm, enabling the formation of faceted snow. This period was likely crucial for the development of the weak layer. The subsequent period was characterized by heavy precipitation, reaching 70 cm at the Magurka station. Strong winds may also have played an important role by transporting the accumulated snow to the leeward side of the mountains. This combination of weak faceted layers overlain by a large amount of new snow created ideal conditions for such a catastrophic avalanche event.

4.2 Identification of potential release areas

An important component of the PRA calculation is

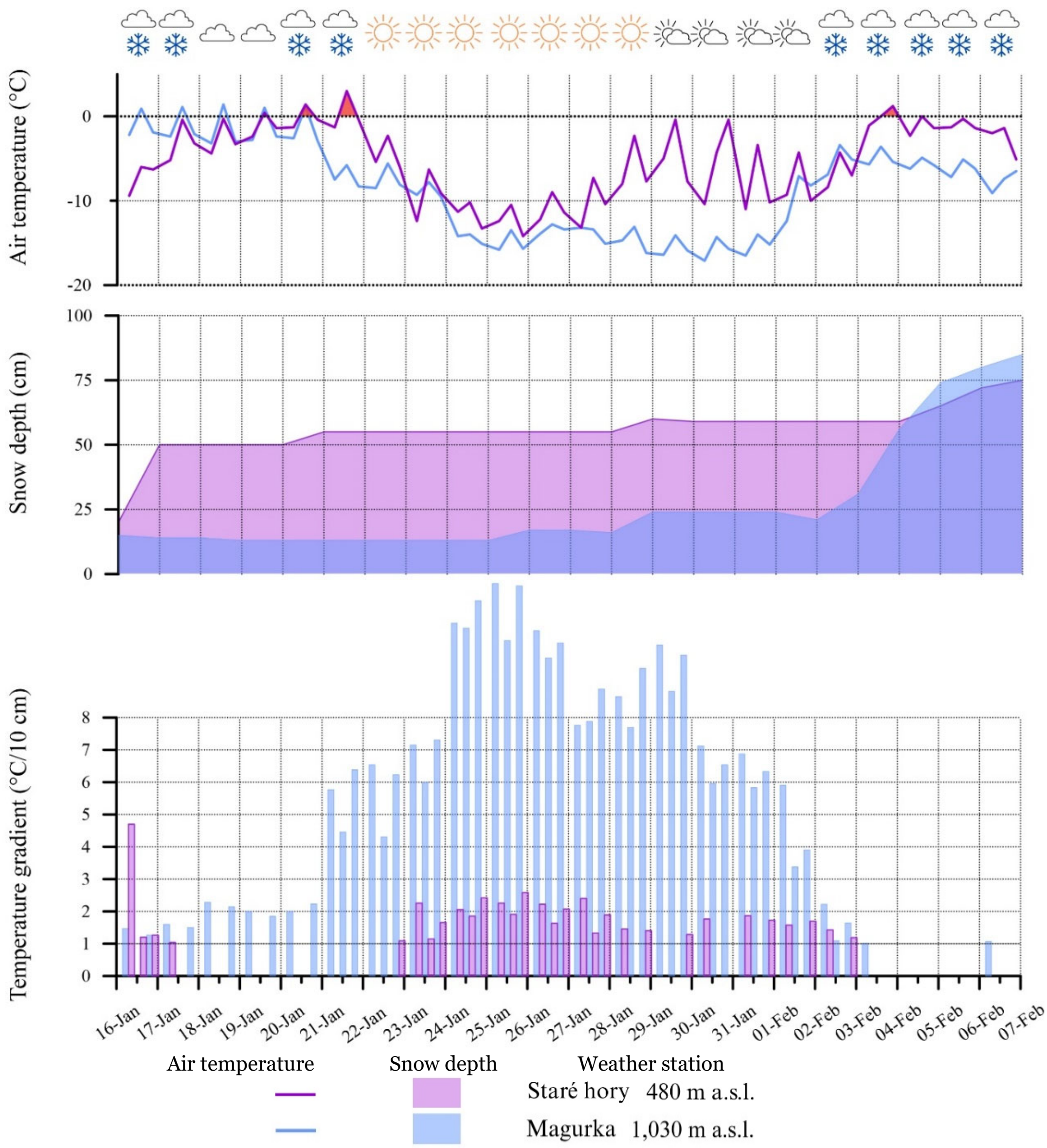

Fig. 7 Development of temperature, snow depth, and temperature gradient at the Staré Hory and Magurka meteorological stations.

the wind-shelter parameter, which simulates the influence of wind on snow distribution. A prevailing wind direction of 315° (northwest) was applied, as this direction is generally the most common in Slovakia during the winter period. It was also recorded as the predominant wind direction in January and February 1924 (Mikulova et al. 2024).

Another important component of the PRA calculation is the percentage of canopy cover. A dense canopy of evergreen conifers is considered to provide the most effective protective function of forests against avalanche release (Perzl et al. 2022). Canopy cover directly affects the radiation balance and influences the development of weak snow layers. It also serves as an indicator of the amount of snowfall intercepted by trees before reaching the snowpack (Bebi et al. 2009). Furthermore, forest canopies limit wind-driven snow transport, thereby reducing the formation of wind slabs.

Percent canopy cover is commonly defined as the proportion of ground area shaded or obscured by tree canopies when viewed from above. It can be estimated using several methods, including aerial imagery, satellite imagery, and remote other sensing techniques. In the model developed by Toft et al. (2024a), this parameter is defined on a scale ranging from 0 to 100. In this study, canopy cover was derived from the previously mentioned historical aerial imagery. The resulting raster map was resampled to a 5 × 5 m resolution. This layer was subsequently used as input for further PRA calculations.

A continuous raster map with values ranging from 0 (not likely) to 1 (very likely) was generated by the algorithm. However, avalanche simulation software typically requires a binary layer in which 0 indicates no avalanche potential and 1 represents a release zone. Therefore, the continuous PRA output was converted into a binary format. It is possible to apply a cutoff threshold, whereby all pixels above this value are included in the potential release area for runout modeling. Larsen et al. (2020) used a threshold value of 0.05 in their study. However, Toft et al. (2024a) considered this approach too conservative and adjusted the threshold to 0.15. The threshold value can be modified depending on whether frequent or more extreme avalanche scenarios are of interest. For this reason, a threshold value of 0.15 was also applied in the present study area, following Toft et al. (2024a).

The final PRA layer was filtered, and small pixel clusters were removed. This step was necessary because most of the small polygons in the ATES Benchmark map were delineated as minor non-forested clusters. These areas were considered too small to realistically function as avalanche release zones, particularly when surrounded by dense forest. Consequently, a vector layer of potential release areas was generated. This layer was divided into two parts: one representing the release area of the main avalanche and the other representing the release area of a preceding avalanche originating from the Rizne locality (Fig. 8).

4.3 Modeling of the preceding avalanche in the Rizne locality

The simulation of the catastrophic avalanche in the Hornojelenecká Valley was preceded by the simulation of an avalanche released from the Rizne locality. The avalanche occurred at a considerable distance from the site of the subsequent disaster, and no immediate threat was posed to the settlement of Rybie (Fig. 9). For this simulation, achieving the target deposition parameters was considered essential. These parameters were derived from a contemporary article

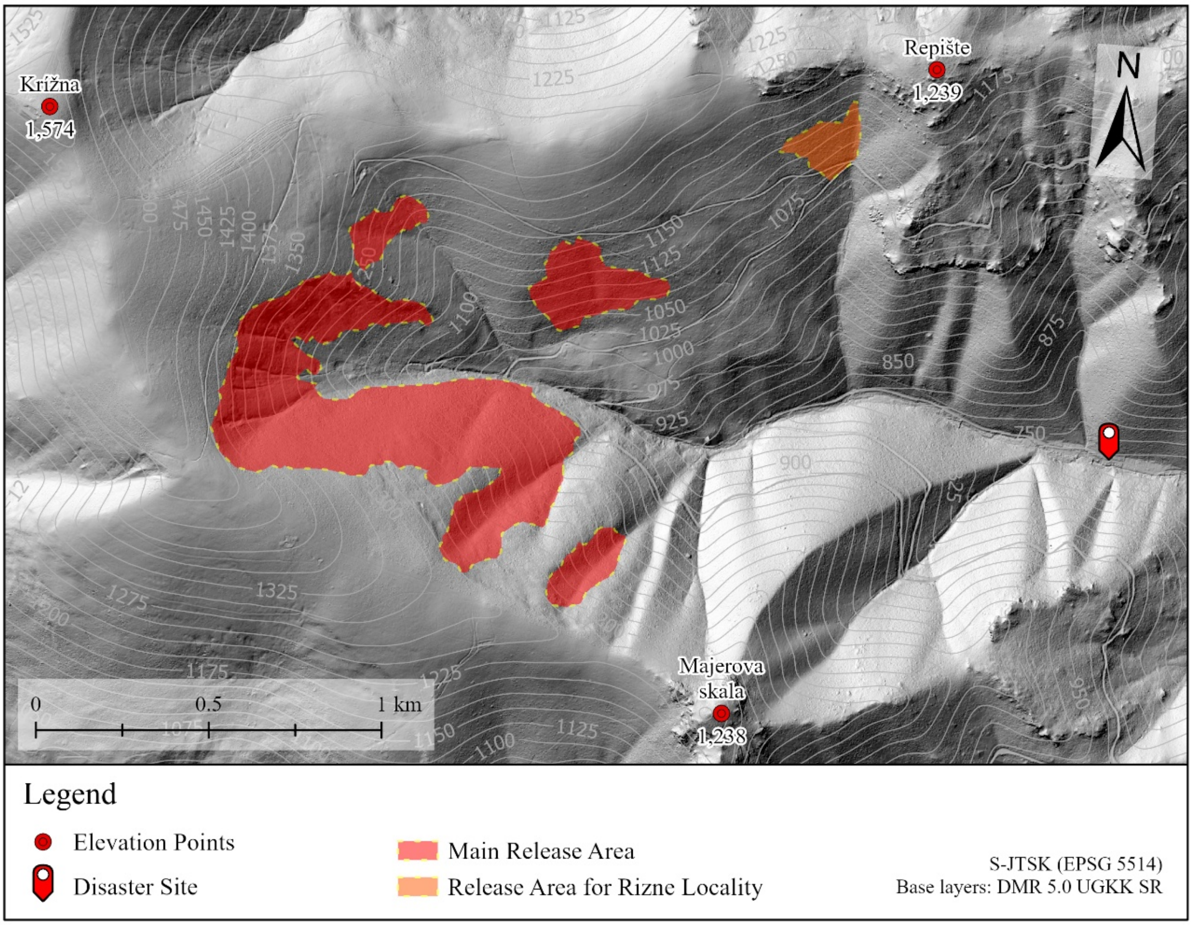

Fig. 8 Potential release areas identified in the Hornojelenecká Valley above the site of the tragic event.

published in the *Karpathen-Post*, which described an avalanche released from below the summit at an elevation of 1,239 m a.s.l. (Repište Peak – Fig. 9). The avalanche was reported to have been approximately 1 km in length, with a width ranging from 50 to 100 m. At the bottom of the Hornojelenecká Valley, a deposit with an approximate thickness of 8 m was formed. Such a deposit thickness was considered plausible in a narrow valley and was likely to have constituted an obstacle to the flow of the main avalanche. Therefore, reproducing a deposit with the specified thickness was established as the primary objective of the simulation.

This simulation was also carried out using both the AvaFrame com1DFA and RAMMS::Avalanche modules. The parameter values for the simulation processes were set according to Table 2.

Under the default settings of the AvaFrame com1DFA module, the required deposit thickness was achieved with a release depth (avalanche crown height) of only 1.00 m. In the RAMMS::Avalanche environment, variable friction parameters were applied, but the required deposit thickness was attained only when a release depth of 1.60 m was used. The possibility of achieving the target deposit with smaller release depths was also tested under constant friction parameters; however, the desired result was not obtained. Nevertheless, given the perpendicular orientation of the Rizne locality relative to the prevailing wind direction, a larger release depth was considered plausible. Furthermore, the objective of the simulation in this case was not to determine the exact release depth, but to ensure the formation of a deposit acting as a barrier with the required characteristics in the valley.

Table 2 Values of input parameters for modeling

Parameter	AvaFrame com1DFA	RAMMS:: Avalanche
Avalanche size (m^3)	Large (> 60,000)	Medium (25 - 60,000)
Density (kg/m^3)	200.00	300.00
Friction parameter μ	Default	Variable
Friction parameter ξ	Default	Variable
Cohesion (Pa)	Default	50.00

The outputs of both models were represented by two separate raster layers depicting the final deposit thickness. Although similar maximum values were achieved for both deposits, their spatial extent differs slightly (Fig. 9). These raster data were subsequently incorporated into the original DTM. In the deposit area, the DTM was modified accordingly, with the deposit

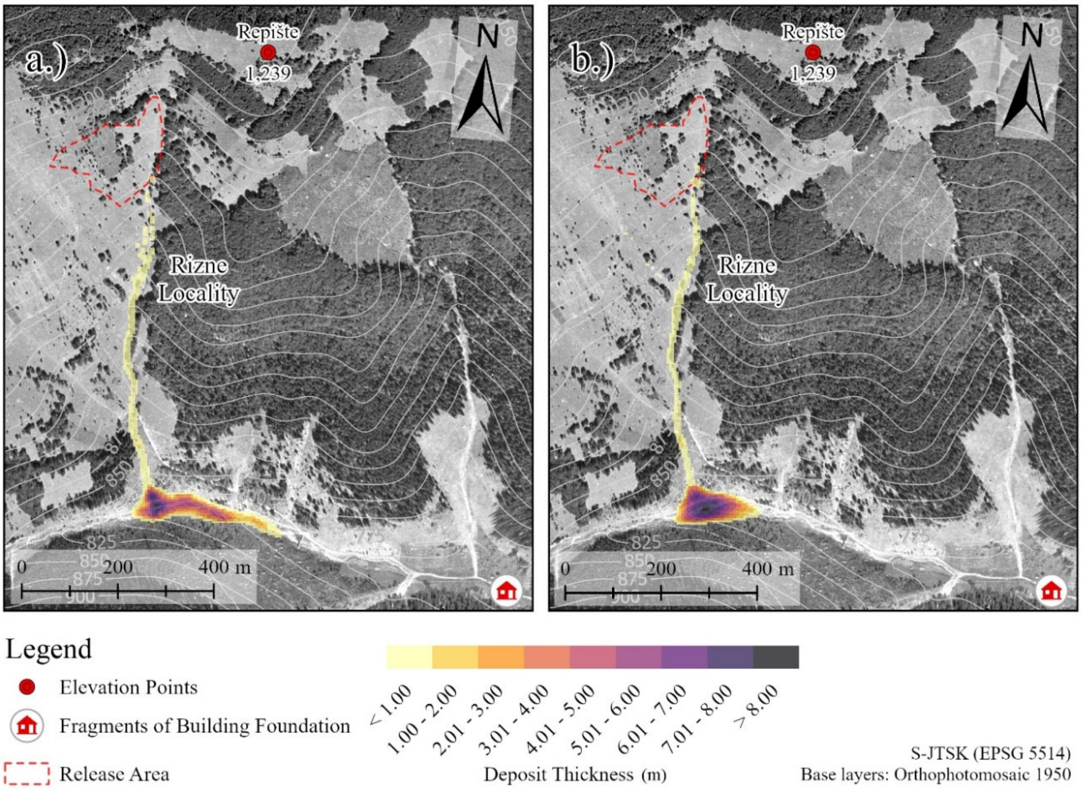

Fig. 9 Deposit thickness in the Rizne locality: (a) result from the AvaFrame com1DFA; (b) result from the RAMMS::Avalanche.

included as an artificial terrain feature. The modified DTMs were then used as inputs for the simulation of the main avalanche.

4.4 Main avalanche modeling

The primary inputs for the simulation of the main avalanche consisted of the release areas and the modified DTMs generated during the previous steps. Independent simulations were conducted using both the AvaFrame and RAMMS environments, following a similar approach to that applied in the Rizne locality. The objective of the simulations was to reproduce an avalanche capable of exerting sufficient deformational forces to cause significant structural damage at the location of the present-day building remains. To achieve this, a series of simulations was performed. The outputs of each simulation consisted of a set of raster-based models, including maximum values of pressure, flow thickness, and velocity, as well as the thickness and extent of the resulting deposit.

To identify the most probable scenario, the primary criterion was defined as the pressure exerted at the location of the buildings rather than the extent of the deposit. The critical pressure value was determined based on the study by Barbolini et al. (2004) and was set at 20 kPa. This value may be subject to discussion, as no records are available from which the exact structural resistance of the affected buildings could be derived. According to Wilhelm (1998), the destruction threshold for reinforced concrete structures is approximately 34 kPa. However, the buildings affected in the settlement of Rybie were not constructed of reinforced concrete. In this case, one brick house, two wooden houses, and several farm buildings were destroyed by the avalanche, while two additional structures were severely damaged. For this reason, the threshold value was set at 20 kPa.

Simulations with the AvaFrame com1DFA module were conducted using constant parameter settings, which are preconfigured for large-type avalanches (Table 2). The default setup of the module is designed to target very large to extremely large avalanches of catastrophic intensity (Tonnel et al. 2023). In the case of the RAMMS::Avalanche module, however, adjustments to the input parameter settings were required. Unlike the Rizne locality, constant friction parameter settings had to be applied in this case. Under variable parameter settings, the simulated avalanche did not reach the observed runout extent of the event, even at the highest tested crown heights. The constant friction parameters were derived from the generated Mu and Xi files, which were used as the basis for their definition. These files were generated based on the default settings for a large avalanche volume type with a 300-year return period. Subsequently, the μ parameter was set to 0.17, and the ξ parameter was set to 2,300. These values were identified as dominant along the entire potential avalanche path based on a weighted average derived from the generated Mu and Xi files. This generalization was also applied to reflect the terrain conditions, which are largely influenced by the frequent occurrence of avalanches, resulting in certain surface smoothing and the absence of forest cover. An approach involving the calibration of the RAMMS::Avalanche module using constant friction parameters represents an alternative solution for achieving optimal results. This approach has been successfully applied in several studies (e.g., Martini et al. 2023; Teich et al. 2014). The preset values used for generating variable friction parameter files may not fully correspond to a specific site, even though they are derived from numerous real avalanche events in alpine environments (Christen et al. 2017).

The subsequent simulations were conducted with the crown height as the only varied parameter. The initial crown height was set to 1.00 m, and the final crown height to 2.00 m. This range of values was determined based on an analysis of meteorological developments and recorded precipitation totals (Section 4.1). In total, 11 simulations, with 10 cm increments, were performed in each modeling environment.

From each simulation, the outputs representing the maximum dynamic pressures within the avalanche flow were further analyzed. These pressure values were spatially evaluated in relation to the locations of the remaining building foundations. The analysis was performed using the Extract Values to Points tool with the bilinear interpolation method in the ArcGIS Pro (Esri) environment. Consequently, the resulting pressure values represent weighted averages of the four nearest cell centers surrounding each target location (Table 3). This approach was selected because the exact shape of the buildings and the way they were impacted are unknown.

The results indicate that, in both simulation modules, the critical pressure value of 20 kPa was exceeded at a crown height of 1.60 m. The pressure fields presented in Fig. 10 exhibit a similar pattern in both models, with the building locations being affected

Table 3 Interpolated pressure values at the location of the remaining building foundations of different crown height

Modelings	Interpolated pressure values (kPa)										
	1.00	1.10	1.20	1.30	1.40	1.50	1.60	1.70	1.80	1.90	2.00
AvaFrame com1DFA	0.00	0.00	2.23	10.81	16.10	18.15	20.94	27.99	37.11	46.55	54.69
RAMMS:: Avalanche	0.00	0.00	0.00	0.00	4.33	7.77	23.20	38.09	53.18	66.51	75.67

at comparable pressure levels (Table 3). At lower crown heights, the site would not have been impacted, or the impact would likely not have resulted in significant structural damage (Table 3). Therefore, a crown height of 1.60 m is considered the probable minimum average release depth for the catastrophic avalanche in the settlement of Rybie.

Simulations with a release depth of 1.60 m were subjected to mutual comparison (Table 4). To verify the results, the outputs were subsequently compared with historical records, including avalanche reach, total avalanche length, deposit length, and deposit thickness. This comparison is presented in Section 6 (Discussion). The simulation results (Table 4) indicate variations in avalanche dynamics; however, the resulting destructive effects at the study site, as well as the overall avalanche reach, were found to be similar.

Table 4 Basic simulation results for a crown height of 1.60 m

Parameter	AvaFrame com1DFA	RAMMS:: Avalanche
Avalanche length (m)	2,864.00	2,937.00
Avalanche area (m^2)	1,032,325.00	1,043,225.00
Max. deposit thickness (m)	27.66	20.85
Overall max. velocity (m/s)	43.50	43.76
Overall max. flowheight (m)	44.07	49.95
Overall max. pressure (kPa)	378.51	574.58

5 Discussion

In temperate-zone mountain regions (such as the Carpathians), diurnal recrystallization is most favorable during clear, cold winter nights. A similar weather pattern was also observed in the study area (Fig. 7). It is driven by strong longwave radiation losses from the snow surface, especially when followed by clear but still subfreezing days. Low-density surface snow enhances this process by providing large pore spaces, which promote strong temperature gradients between adjacent grains, increased vapor transport, and the growth of faceted crystals. Under such conditions, extreme temperature gradients have been observed (e.g., Fukuzawa and Akitaya 1993; Birkeland et al. 1998). Nocturnal temperature gradients are negative, whereas diurnal gradients are positive, producing bidirectional faceting of snow crystals (Birkeland 1998).

Faceted forms at and near the surface develop rapidly under high temperature gradients. Near-surface faceted layers are another form, like surface hoar, that is of primary importance in avalanche studies. They represent a type of persistent weak layer that can remain for long periods and are responsible for major avalanches and numerous fatalities during backcountry travel. Near-surface faceted layers, surface hoar, and combinations of these forms associated with crusts constitute persistent weak layers that are critically important in determining avalanche hazards in backcountry terrain. Depth hoar is also considered a persistent form; however, it does not exhibit the same prominence as the other types in reported major accidents. The back-analysis of weather conditions and snowpack characteristics thus highlights their critical importance for the course of this tragic event.

Based on several studies (e.g. Larsen et al. 2020; Toft et al. 2024a), the applied approach for identifying potential release areas can generally be considered relatively reliable. However, in the case of this study, a certain degree of uncertainty must be taken into account. This uncertainty arises from the historical nature of the event, which is associated with the absence of more precise data for validation of the results. For the most accurate simulation, it is ideal to map avalanche release areas (their spatial extent and depth) and snowpack characteristics in situ immediately after the event (Frigo et al. 2021). However, this is not possible in the reconstruction of a historical event. This degree of uncertainty is therefore propagated throughout the entire modeling process. Moreover, the use of simulation models is typically associated with a calibration process with respect to local conditions. With a limited input data basis, this process can be considerably challenging.

On the other hand, historical records describing the impacts of this avalanche event provide a certain framework for validation. The relevance of the results is further supported by the application of two independent simulation tools. Their outputs, in the form of pressure models (Fig. 10), closely approach the

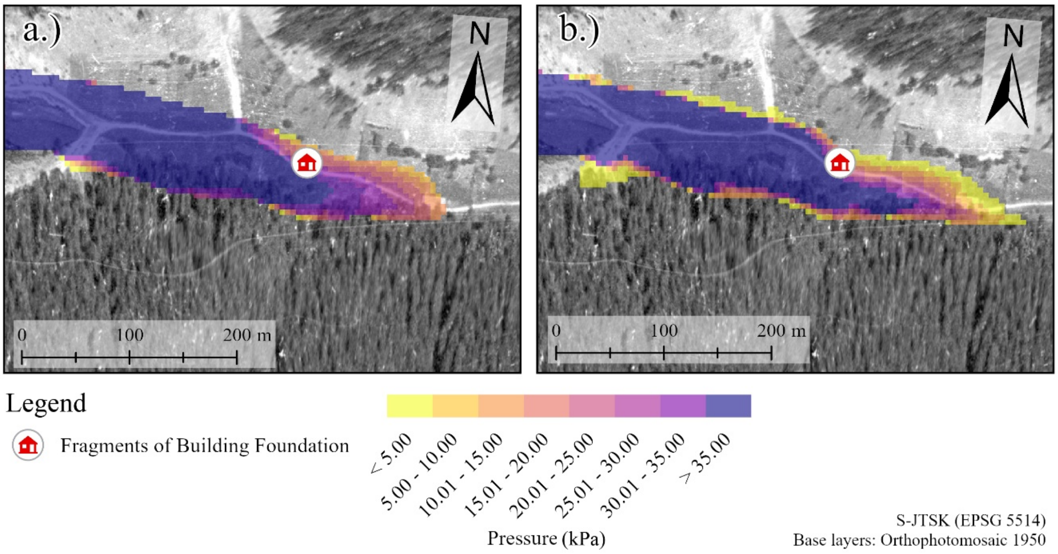

Fig. 10 Pressure model at the location of the affected building for a crown height of 1.60 m: (a) model from AvaFrame com1DFA; (b) model from RAMMS::Avalanche.

defined critical value at a crown height of 1.60 m. At this crown height, both simulations also show relatively good agreement with historical records in other aspects.

The credibility of both simulations is further supported by the overall avalanche reach. In both cases, the avalanche was extended sufficiently to produce destructive effects at the targeted building. At the same time, no additional flow into the settlement, which would likely have caused further structural damage and been documented, was simulated by either model. A difference of only 73 m in avalanche length was observed between the two models (Fig. 10).

The total length of the simulated avalanches, measured from the highest release point to the front of the deposit, was approximately 2,900 m. A length of approximately 2,500 m was reported in historical records. However, this discrepancy cannot be considered entirely conclusive, as it may have been substantially influenced by the methods and accuracy employed in the historical measurements.

A similar situation is observed for the deposit length parameter. Deposits generated by the models begin at thicknesses of just a few millimeters, which cannot be directly compared with actual terrain conditions. Therefore, a certain degree of generalization is required. When considering deposits thicker than 1 m, the total length in both models fluctuates around 1,800 m, whereas historical records indicate a length of approximately 1,500 m. This represents another minor discrepancy. In the upper section of the avalanche, the deposits form only narrow infill zones along the valley floor, as observed in both models (Fig. 11). Such areas could have easily been overlooked in the field and consequently not included in the total measured deposit length.

Another control parameter is deposit thickness, which is described in historical records as ranging between 10 and 25 m. However, these values are considered rather imprecise; therefore, it is more appropriate to focus on maximum deposit thickness. The deposit model generated by AvaFrame com1DFA reaches its maximum thickness at the location where it intersects with the deposit of the preceding avalanche from the Rizne locality. In these areas, the model locally exceeds a deposit thickness of 25 m (Fig. 11a). A similar situation is observed in the RAMMS::Avalanche model; however, in this case, the maximum deposit thickness reaches only about 21 m (Fig. 11b). The mitigating effect of the preceding avalanche is evident in both simulations, as confirmed by historical records and previous studies (e.g., Bartík and Richnavský 2015).

Despite the noted differences and the associated degree of uncertainty, both models can generally be considered plausible. The results correspond closely with historical records and, at the same time, provide a range of new insights and parameters regarding the probable course of this catastrophic event.

6 Conclusions

The results of this study highlight the strong

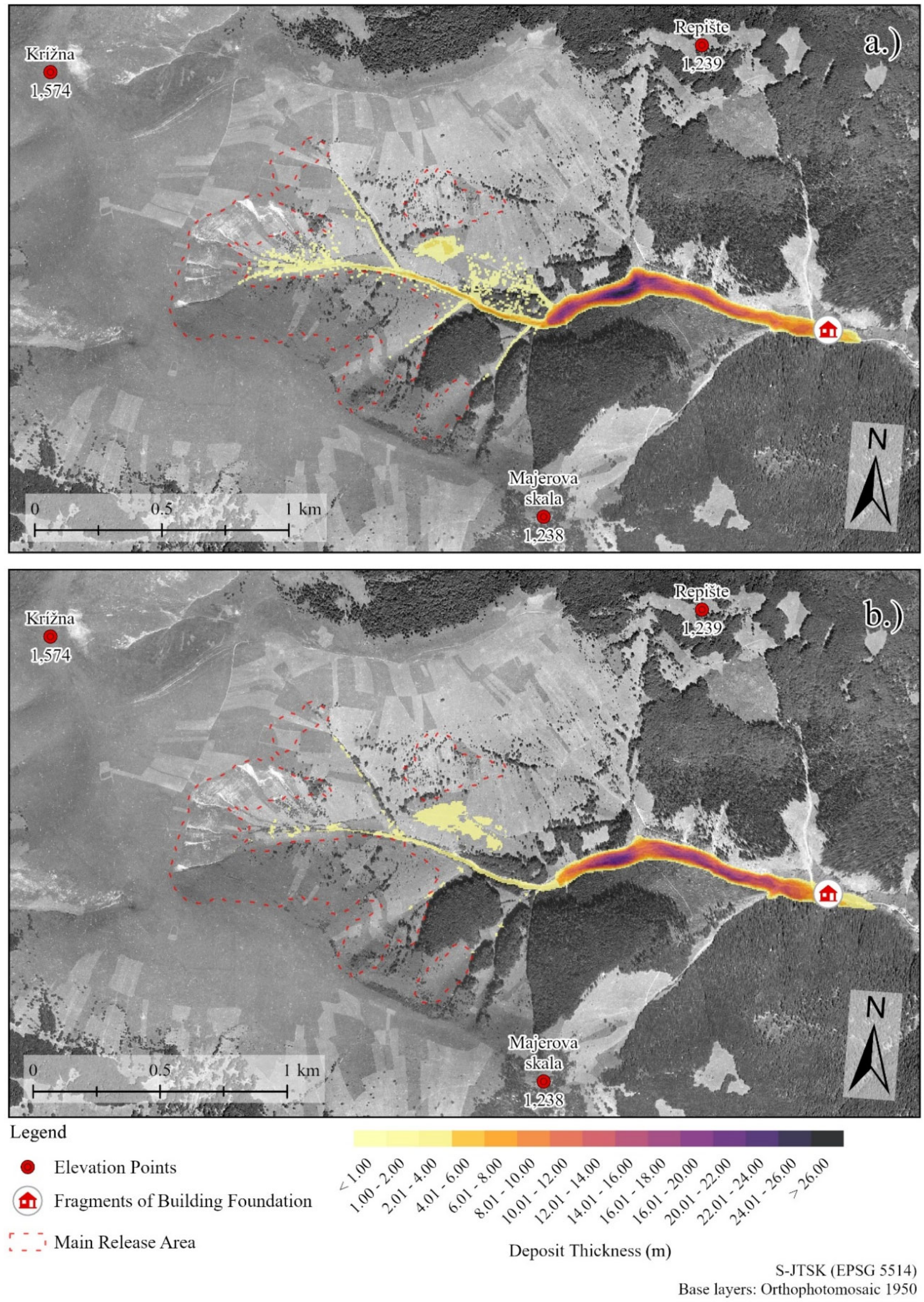

Fig. 11 Final avalanche deposit: (a) result from the AvaFrame com1DFA; (b) result from the RAMMS:: Avalanche.

potential of modeling and GIS tools for the back-analysis of avalanche events. The application of modern approaches and tools was demonstrated to be feasible even for historical events, where the availability of input data may be significantly limited. This was the case in the simulation of the most catastrophic avalanche event in Slovakia (and the Western Carpathians), which occurred in 1924 in the settlement of Rybie. Based on historical records of meteorological conditions during this period, the approximate evolution of snowpack characteristics was reconstructed. Building on the previously identified potential release areas, a series of simulations was conducted, enabling the determination of the probable minimum average crown height that resulted in the catastrophic avalanche. A key component of this analysis was the assessment of the avalanche's destructive effects at the locations of the remaining building foundations. Two different simulation tools were employed, each based on distinct physical principles and utilizing different sets of input parameters. However, for certain parameter values, the outputs were found to be nearly identical, indicating a high probability of the resulting scenario.

The identification of potential release areas and the determination of the probable minimum average crown height represent a significant contribution to historical records. Based on these findings, the course of the entire event can be reconstructed with greater accuracy. However, a certain degree of uncertainty must be taken into account when interpreting the results. Their validation is partially limited due to the historical nature of the event. Moreover, the obtained results have implications beyond the local context, as the presented approaches can be applied more broadly in the field of avalanche accident reconstruction.

Acknowledgments

The authors received no specific funding for this work.

Author Contributions

All authors contributed equally to the study and participated in every stage of the creative process, from conceptualization to implementation.

Ethics Declarations

Availability of Data/Materials: The datasets generated during this study are available from the corresponding author upon reasonable request, in accordance with cooperation agreements and scientific research project frameworks.

Conflict of Interest: The authors declare that they have no conflicts of interest.

Open Access

Funding note: Open access funding provided by The Ministry of Education, Science, Research and Sport of the Slovak Republic in cooperation with Centre for Scientific and Technical Information of the Slovak Republic.

References

Adams EE, Brown RL (1983) Metamorphism of dry snow as a result of temperature gradient and vapor density differences. Ann Glaciol 4: 3-9. https://doi.org/10.3189/S0260305500005140

Bartík M, Richnavský J (2015) Reconstruction of the most tragic avalanche in Slovakia with using RAMMS and ELBA+. In: Longauer M, Bartík M, Škvarenina J (eds.), 90th anniversary of the most tragic avalanche in Slovakia, Rybie, Veľká Fatra: Proceedings of the scientific conference held on February 4, 2014, at the Technical University in Zvolen. Zvolen: Technical University in Zvolen. 150 pp. ISBN 978-80-228-2850-5 (In Slovak).

Barbolini M, Cappabianca F, Sailer R (2004) Empirical estimate of vulnerability relations for use in snow avalanche risk assessment. In: Brebbia CA (ed.), Proceedings of the 4th International Conference on Computer Simulation in Risk Analysis and Hazard Mitigation "Risk Analysis 2004", 27-29 September, Rhodes, Greece, WIT Press. pp 533-542.

Bebi P, Kulakowski D, Rixen, C (2009) Snow avalanche disturbances in forest ecosystems - State of research and implications for management, Forest Ecol Manage 257: 1883-1892. https://doi.org/10.1016/j.foreco.2009.01.050

Birkeland KW (1998) Terminology and predominant processes associated with the formation of weak layers on NearSurface Faceted Crystals in the Mountain Snowpack. Arct Alp Res 30: 193-199.

Birkeland KW, Johnson RE, Schmidt DS (1998) Near-surface faceted crystals formed by diurnal recrystallization: A case study of weak layer formation in the mountain snowpack and its contribution to snow avalanches. Arct Alp Res 30: 200-204.

Bergua SB, Piedrabuena MÁP, Marino AJL (2019) Snow avalanches, land use changes, and atmospheric warming in landscape dynamics of the Atlantic Mid-Mountains (Cantabrian Range, NW Spain). Appl Geogr 107: 38-50. https://doi.org/10.1016/j.apgeog.2019.04.007

Bukovčan, V (1960) Avalanches and Forests. Bratislava: Slovak Agricultural Literature Publishing House, 199 p. (In Slovak)

Bühler Y, Kumar S, Veitinger J, et al. (2013) Automated identification of potential snow avalanche release areas based on digital elevation models. Nat Hazards Earth Syst Sci 13: 1321-1335. https://doi.org/10.5194/nhess-13-1321-2013

Colbeck SC (1982) An overview of seasonal snow meta-morphism. Rev Geophys Space Phys 20(1): 45-61. https://doi.org/10.1029/RG020i001p00045

Eckert N, Corona C, Giacona F, et al. (2024) Climate change impacts on snow avalanche activity and related risks. Nat Rev Earth Environ 5: 369-389. https://doi.org/10.1038/s43017-024-00540-2

Eckert N, Coleou C, Castebrunet H, et al. (2010) Cross-comparison of meteorological and avalanche data for characterising avalanche cycles: The example of December 2008 in the eastern part of the French Alps. Cold Reg Sci Technol 64 (2): 119-136. https://doi.org/10.1016/j.coldregions.2010.08.009

Frigo B, Bartelt P, Chiaia B, et al. (2021) A reverse dynamical investigation of the catastrophic wood-snow avalanche of 18 January 2017 at Rigopiano, Gran Sasso National Park, Italy. Int J Disaster Risk Sci 12: 40-55. https://doi.org/10.1007/s13753-020-00306-6

Fukuzawa T, Akitaya E (1993) Depth-hoar crystal growth in the surface layer under high temperature gradient. Ann Glaciol 18: 39-45. https://doi.org/10.3189/S026030550001123X

García-Hernández C, Ruiz-Fernández Ch, Sánchez-Posada C, et al. (2017) Reforestation and land use change as drivers for a decrease of avalanche damage in mid-latitude mountains (NW Spain). Glob Planet Change 153: 35-50. https://doi.org/10.1016/j.gloplacha.2017.05.001

Christen M, Kowalski J, Bartelt P (2010) RAMMS: numerical simulation of dense snow avalanches in three-dimensional terrain. Cold Reg Sci Technol 63: 1-14. https://doi.org/10.1016/j.coldregions.2010.04.005.

Christen M, Bartelt P, Bühler Y, et al. (2017) RAMMS User Manual v1.7.0.: A Modeling System for Snow-Avalanches in Research and Practice; WSL Intitute for Snow and Avalanche Research: Birmensdorf, Switzerland. p 104.

Jamieson B, Geldsetzer T, Stethem C (2001) Forecasting for deep slab avalanches. Cold Reg Sci Technol 33: 275-290. https://doi.org/10.1016/S0165-232X(01)00056-8

Karpathen-Post (1924) Vol. 45, Issue No. 9 Kežmarok - Kesmark, Available at: https://www.difmoe.eu/view/uuid:f678f1b4-7dd4-4703-b78d-201903564edb?page=uuid:8725be47-6771-4206-a842-d809f998e1ad

Kňazovický L (1979) Atlas of Avalanche Paths of the Slovak Socialist Republic. HS SÚV ČSZTV a SŠP, 1979. p 37. (In Slovak)

LaChapelle ER, Armstrong RL (1977) Temperature patterns in an alpine snow cover and their influence on snow metamorphism. Technical Report. Inst, for Arctic and Alpine Res., Univ, of Colorado, Boulder. p 42.

Larsen HT, Hendrikx J, Slåtten MS, et al. (2020) Developing nationwide avalanche terrain maps for Norway. Nat Hazards 103: 2829-2847.

Liščák P, Biskupič M, Richnavský J, et al. (2017) Geological hazards. In: Dalezios NR (ed.), Environmental Hazards Methodologies for Risk Assessment and Management. ISBN: 9781780407135.

Longauer M (2015) State and assessment of first biological and technical avalanche barriers at the eastern slopes of Krížna after 50 years. In: Longauer M, Bartík M, Škvarenina J (eds.), 90th anniversary of the most tragic avalanche in Slovakia, Rybie, Veľká Fatra: Proceedings of the scientific conference held on February 4, 2014, at the Technical University in Zvolen. Zvolen: Technical University in Zvolen. p 150. ISBN 978-80-228-2850-5 (In Slovak)

Maggioni M, Gruber U (2003) The influence of topographic parameters on avalanche release dimension and frequency. Cold Reg Sci Technol 37: 407-419. https://doi.org/10.1016/S0165-232X(03)00080-6

Mayer S, Hendrick M, Michel A, et al. (2024) Impact of climate change on snow avalanche activity in the Swiss Alps. The Cryosphere 18: 5495-5517. https://doi.org/10.5194/tc-18-5495-2024

McClung DM, Schaerer PA (1993) The Avalanche Handbook. Seattle, WA, The Mountaineers. p 272.

Mikulova K, Vojtek M, Ivaňáková G, et al. (2024) Analysis of the meteorological conditions of the most tragic avalanche in Slovakia on 6th February 1924 in Rybô (Veľká Fatra Mountains). Meteorol J 27: 3 - 11. (In Slovak)

Martini M, Baggio T, D'Agostino V (2023) Comparison of two 2-D numerical models for snow avalanche simulation. Sci Total Environ 896. https://doi.org/10.1016/j.scitotenv.2023.165221

Miller A, Sirguey P, Morris S, et al. (2022) The impact of terrain model source and resolution on snow avalanche modeling. Nat Hazards Earth Syst Sci 22: 2673-2701. https://doi.org/10.5194/nhess-22-2673-2022

Oesterle F, Wirbel A, Fischer JT, et al. (2025) Avaframe/ AvaFrame 1.13.1. Zenodo. https://doi.org/10.5281/zenodo.16979398

Ortner G, Michel A, Spieler MBA, et al. (2025) A novel approach for bridging the gap between climate change scenarios and avalanche hazard indication mapping. Cold Reg Sci Technol 230. https://doi.org/10.1016/j.coldregions.2024.104355

Perzl F, Bono A, Garbarino M, et al. (2022) Protective effects of forests against gravitational natural hazards. In: Teich M, Accastello C, Perzl F, et al. (Eds.) Protective Forests as Ecosystem-based Solution for Disaster Risk Reduction (Eco-DRR). IntechOpen. https://doi.org/10.5772/intechopen.99506

Schweizer J, Mitterer Ch, Stoffel L (2009) On forecasting large and infrequent snow avalanches. Cold Reg Sci Technol 59(2-3): 234-241.https://doi.org/10.1016/j.coldregions.2009.01.006

Sharp E (2018) Evaluating the exposure of heliskiing ski guides to avalanche terrain using a fuzzy logic avalanche susceptibility model, Master's Thesis, University of Leeds, School of Geography, Leeds. p 88. https://doi.org/10.13140/RG.2.2.18673.94567

Slivinski LC, Compo GP, Whitaker JS, et al. (2019) Towards a more reliable historical reanalysis: Improvements for version 3 of the Twentieth Century Reanalysis system. QJR Meteorol Soc 145: 2876-2908. https://doi.org/10.1002/qj.3598

Sykes J, Toft H, Haegeli P, Statham G (2024) Automated Avalanche Terrain Exposure Scale (ATES) mapping - local validation and optimization in western Canada. Nat Hazards Earth Syst Sci 24: 947-971. https://doi.org/10.5194/nhess-24-947-2024

Teich M, Fischer JT, Feistl T, et al. (2014) Computational snow avalanche simulation in forested terrain. Nat Hazards Earth Syst Sci 14: 2233-2248. https://doi.org/10.5194/nhess-14-2233-2014

Toft HB, Sykes J, Schauer A, et al. (2024a) AutoATES v2.0: Automated Avalanche Terrain Exposure Scale mapping. Nat Hazards Earth Syst Sci 24: 1779-1793. https://doi.org/10.5194/nhess-24-1779-2024

Toft HB, Sykes JM, Schauer A (2024b) AutoATES-v2.0, GitHub [code]. https://github.com/AutoATES (last access: 19 January 2024).

Tonnel M, Wirbel A, Oesterle F, et al. (2023) AvaFrame com1DFA (v1.3): a thickness-integrated computational avalanche module - theory, numerics, and testing. Geosci Model Dev 16: 7013-7035. https://doi.org/10.5194/gmd-16-7013-2023

Valero CV, Jones KW, Bühler Y, et al. (2015) Release temperature, snow-cover entrainment and the thermal flow regime of snow avalanches. J Glaciol 61(225): 173-184. https://doi.org/10.3189/2015JoG14J117

Veitinger J, Purves RS, Sovilla B (2016) Potential slab avalanche release area identification from estimated winter terrain: a multi-scale, fuzzy logic approach. Nat Hazards Earth Syst Sci 16. https://doi.org/10.5194/nhess-16-2211-2016

Vojtek M (2015) Meteorological conditions preceding the burial of the Rybô village by an avalanche on 6th Feb 1924. In: Longauer M, Bartík M, Škvarenina J (eds.), 90th anniversary of the most tragic avalanche in Slovakia, Rybie, Veľká Fatra: Proceedings of the scientific conference held on February 4, 2014, at the Technical University in Zvolen. Zvolen: Technical University in Zvolen. p150. ISBN 978-80-228-2850-5 (In Slovak)

Wilhelm C (1998) Quantitative risk analysis for evaluation of avalanche protection projects. In: Hestness (ed.), Proc. of 25 Years of Snow Avalanche Research at NGI, Voss 12-16 May 1998, NGI Publications 203, Oslo. pp 288-293.